# Peer Community Journal

Section: Ecotoxicology and Environmental Chemistry

Research article

**Published** 2025-11-12

Cite as

Chan Gao, Hélène Budzinski,
Patrick Pardon, Karyn Le
Menach and Pierre Labadie
(2025) Investigation of the
combined influence of salinity
and particle concentration on
the adsorption of anionic and
zwitterionic PFAS onto estuarine
sediment using the RSM
modelling approach, Peer
Community Journal, 5: e124.

#### Correspondence

pierre.labadie@u-bordeaux.fr

#### Peer-review

Peer reviewed and recommended by PCI Ecotoxicology and Environmental Chemistry, https://doi.org/10.24072/pci. ecotoxenvchem.100249



This article is licensed under the Creative Commons Attribution 4.0 License.

Investigation of the combined influence of salinity and particle concentration on the adsorption of anionic and zwitterionic PFAS onto estuarine sediment using the RSM modelling approach

Chan Gao<sup>1</sup>, Hélène Budzinski<sup>0,1</sup>, Patrick Pardon<sup>0,1</sup>, Karyn Le Menach<sup>1</sup>, and Pierre Labadie<sup>0,1</sup>

Volume 5 (2025), article e124

https://doi.org/10.24072/pcjournal.645

# **Abstract**

Salinity (S) and suspended particulate matter (SPM) are key factors influencing the sorption of micropollutants in estuaries, due to strong gradients in these ecosystems. Previous laboratory or field-based studies have typically investigated the impact of S or SPM separately. Thus, the combined effects of S and SPM as well as their interactions on the sorption of micropollutants such as per- and polyfluoroalkyl substances (PFAS) in estuarine environments still remain poorly understood. We initially investigated the adsorption kinetics of 11 anionic and zwitterionic PFAS onto estuarine sediment under one S/SPM combination in laboratory-controlled conditions, as well as their adsorption isotherms under two S/SPM combinations. We also determined their distribution coefficients (K<sub>d</sub>) across 35 S/SPM combinations covering a wide range of estuarine conditions. The adsorption kinetics of PFAS could be described by a pseudo-second-order model (equilibrium time <24h). Sorption isotherms were fitted by both linear and Freundlich models; the linear sorption range was in the range 0.12-1.31 nM and  $K_d$  varied between 0.6 and 55271 L/kg. Based on response surface modelling, both S and SPM were significant factors, i.e. K<sub>d</sub> was positively related to S (salting-out effect), while it was negatively related to SPM concentration (third-phase effect). SPM had a stronger effect than S for short-chain carboxylates, whereas S was the dominant factor for most other compounds. We also present, for the first time, evidence of a significant negative interaction between these two factors. This study therefore provides a new perspective to model the fate of PFAS at the land-sea interface.

<sup>1</sup>Univ. Bordeaux, CNRS, Bordeaux INP, EPOC, UMR 5805, F-33600 Pessac, France





#### Introduction

Per- and polyfluoroalkyl substances (PFAS) have been widely utilized for over 70 years in various industrial sectors, including the fluoropolymer industry, aqueous film-forming foams (AFFFs) or household products (Evich et al., 2022). The fate of PFAS in the aquatic environment has attracted public and scientific attention for the extreme persistence of many of these compounds, their widespread occurrence and their toxic effects (Manojkumar et al., 2023; Zhong et al., 2021). Due to both i) the hydrophobic/lipophobic nature of their fluoroalkyl chain and ii) the charged state of most of these substances, PFAS are expected to interact strongly with sediment particles in aquatic ecosystems (Munoz et al., 2017). This may influence their transport and distribution (Ahmed et al., 2020). Estuarine sediments are considered as a major sink for PFAS (Feng et al., 2020), and sediment-water interactions under estuarine conditions are considered a crucial process in determining the distribution and fate of micropollutants at the land-sea interface (Bowman et al., 2002). This is a critical issue since a recent study further confirmed the major role of oceans in the global cycling of PFAS (Sha et al., 2022).

The sorption of PFAS onto suspended sediment plays an important role in the fate of these chemicals under estuarine conditions; such interactions are governed by both PFAS properties and environmental factors such as salinity (S) and suspended particulate matter (SPM) concentration (Zhang et al., 2019). PFAS with different properties exhibit different sorption behaviors. Previous studies reported that PFAS characteristics such as chain length (Fabregat-Palau et al., 2021; Sörengård et al., 2020), nature of the functional group (Nguyen et al., 2020; Sörengård et al., 2020) and charged state (Mejia-Avendaño et al., 2020; Xiao et al., 2019) may affect PFAS sorption. For instance, the sorption behavior of legacy PFAS such as perfluoroalkyl acids (PFAAs) (including perfluorocarboxylic acids (PFCAs) and perfluoroalkyl sulfonates (PFSAs)) has been extensively studied (Mejia-Avendaño et al., 2020). For those compounds, hydrophobicity and electrostatic interactions have been regarded as the main driving forces of sorption (Higgins & Luthy, 2006; Du et al., 2014; Sorengard et al., 2019; Nguyen et al., 2020). Previous studies indicated that the length of the PFAA hydrophobic fluoroalkyl chain clearly influences the sorption process (Mejia-Avendaño et al., 2020; Nguyen et al., 2020). For a similar chain length, PFSAs, which bear a sulfonic group, possess a higher adsorptive capacity than PFCAs due to their more hydrophobic structure (Askeland et al., 2020; Butzen et al., 2020). Besides, electrostatic interaction between anionic PFAAs and positively charged adsorbents facilitate sorption (Zhang et al., 2019). However, there is also electrostatic repulsion between anionic PFAAs and negatively charged adsorbents that hinders sorption (Yin et al., 2022). Overall, it is considered that hydrophobicity may be a more prevailing factor compared to electrostatic interaction (Nguyen et al., 2020).

Apart from legacy PFAS, emerging cationic or zwitterionic PFAS such as 8:2 fluorotelomer sulfonamidoalkyl betaines (FTABs) have been detected widely, although reports still remain scarce (Munoz et al., 2016; Meng et al., 2021; Macorps et al., 2023). The sorption of these chemicals appears more complex and difficult to predict, based on the bulk sorbent properties. Meanwhile, there is still a lack of information on the sorption of co-occurring legacy and emerging PFAS with contrasting properties (Yin et al., 2022). Some studies found that the co-occurrence of PFAS species as well as their initial concentrations could influence PFAS sorption (Liu et al., 2022; You et al., 2010). At lower concentration (i.e. <200 nM), the influence of competitive adsorption on isotherms was generally negligible and PFAS isotherms were linear (Liu et al., 2022). At higher concentration, however, competitive adsorption exists between long-chain and short-chain PFAS, i.e. short-chain PFAS are indeed prone to be displaced by long-chain PFAS (Zhang et al., 2023). Thus, estimating the effect of the PFAS initial concentration on sorption isotherms is critical for investigating the sorption behavior of co-occurring PFAS. This clearly contributes to providing more reliable information for evaluating and simulating the fate of PFAS in the environment.

In addition, S and SPM are two prevalent factors affecting the adsorption process in estuaries, due to the large contrasting S and SPM gradients from fresh to seawater (Munoz et al., 2017). Laboratory experiments showed that S had a favorable impact on PFAS sorption, which is partly related to the salting-out effect: an increasing salt concentration decreases the solubility of neutral solutes in water (You et al., 2010). Besides, the linearity of PFAS adsorption isotherm may be affected by salinity because the increase of salt concentration reduces the electrostatic repulsion

between adsorbents and sorbates (Chen et al., 2020). As regards the effect of SPM on sorption, a few experimental studies have shown a decrease of Kd with increasing SPM concentration, owing to the particle-concentration effect (Bowman et al., 2002; Munoz et al., 2017). For instance, a sharp decrease in Kd in the SPM range <0.02-0.5 g L-1 was observed in a field-study by (Munoz et al., 2017). It was hypothesized that such particle-concentration effect might be due to the enhanced aggregation of SPM particles at high concentrations. This causes a drastic decrease of SPM specific surface area, thereby reducing the amount of available sorption sites (Munoz et al., 2017) and causing nonlinear sorption of PFAS (Chen et al., 2020). However, owing to the complex dynamics of S and SPM in estuarine areas, understanding the combined influence of these factors on PFAS sorption remains intricate and data on the particle-water distribution of PFAS under contrasted conditions is still limited. Previous attempts to address this issue primarily relied on field-based data, which, while useful, can sometimes be complex to interpret due to potentially overlooked confounding factors (Munoz et al., 2017). To date, the combined effects of S and SPM, as well as their interactions, on PFAS sorption in estuarine environments have not been investigated under controlled laboratory conditions - an essential requirement for accurately assessing the relative influence of these factors.

Therefore, the main objective of this work was to study the effect of major drivers of PFAS Kd under estuarine conditions, using experiments performed in a laboratory-controlled setting. More precisely, the specific objectives of this work were 1) to determine the sorption kinetics of 11 anionic and zwitterionic PFAS onto a model estuarine sediment; 2) to investigate their sorption isotherms and their linear sorption range; 3) to use response surface methodology (RSM) modeling to investigate the combined influence of S and SPM on PFAS sorption and their interaction effects.

#### Materials and methods

#### Chemicals

As regards quantitative analysis, certified PFAS native standards (n = 11) and isotope-labeled internal standards (ISs) (n = 10) were all obtained from Wellington Laboratories (BCP Instruments, Irigny, France) (chemical purity >98% and isotopic purity >94%). Native PFAS included seven perfluoroalkyl carboxylic acids (PFCAs: PFHxA, PFHpA, PFOA, PFNA, PFDA, PFDA, PFDODA), three perfluoroalkyl sulfonic acids (PFCAs: PFHxA, PFHpA, PFOA, PFNA, PFDA, PFUnDA, PFDoDA), three perfluoroalkyl sulfonic acids (PFSAs: PFHxS, Br-PFOS, L-PFOS) and one polyfluoroalkyl zwitterionic compound (8:2 FTAB). Besides, <sup>13</sup>C<sub>2</sub>-PFHxA, <sup>13</sup>C<sub>4</sub>-PFHpA, <sup>13</sup>C<sub>4</sub>-PFOA, <sup>13</sup>C<sub>5</sub>-PFNA, <sup>13</sup>C<sub>5</sub>-PFUnDA, <sup>18</sup>O<sub>2</sub>-PFHxS, and <sup>13</sup>C<sub>4</sub>-PFOS were used as ISs. Note that herein L-PFOS refers to the linear PFOS isomer and Br-PFOS to the sum of branched PFOS isomers. The concentrations of Br-PFOS were calculated from the calibration curve used for L-PFOS (Munoz et al., 2015, 2017). Please refer to Table S1 and Table S2 in the Supplementary information for more information on the standards and internal standards.

To perform sorption experiments, we used a different set of standards. Pure PFAS (> 98%) standards were supplied by Sigma-Aldrich (St Quentin Fallavier, France) while 8:2 FTAB (>95%) was synthesized by Innovorga (Reims, France). Note that the PFOS standard was actually a technical mixture containing both L- and Br-PFOS (7:3). For these standards, working solutions were prepared in MeOH at 70 ng/mL.

Ammonium acetate (CH₃COONH₄) (7.5 mM aqueous solution), hydrochloric acid (HCl), methanol (MeOH, Ultra gradient HPLC gradient grade) and acetonitrile (ACN, Ultra gradient HPLC gradient grade) were from J.T. Baker (Atlantic Labo, Bruges, France). Supelclean ENVI Carb cartridges (250 mg/3 mL), ammonium hydroxide (NH₄OH) (28.0-30.0 % NH3 basis), sodium hydroxide (NaOH, >98.5%) and ammonium acetate (Fluka) for HPLC (≥ 99.0 %) were obtained from Sigma-Aldrich (St Quentin Fallavier, France). Ultrapure water was obtained using a Millipore Elix 10 system fitted with an EDS Pak polisher. Instant Ocean synthetic sea salt was purchased from Aquarium Systems (France). Nitrogen gas (99.999 %) was from Linde (St Priest, France). Polypropylene (PP) centrifuge tubes (50mL/225 mL) were obtained from Corning, Tewksbury, USA.

#### Sediment and salt solutions

A composite sediment sample (1 kg) was collected from tidal mudflats at Cadaujac, in the upstream area of the Gironde estuary (South West France, 44°45'23"N / 0°31'44"W). Samples were then air-dried, ground to a fine powder with a ball mill, sieved at 63µm, homogenized and stored at room temperature in an amber glass jar. The background concentration of PFAS in this sediment sample was analyzed. The results showed that most PFAS targeted in this study were present, albeit at low levels (< limit of detection–0.37 ng/g dry weight). Details on the sediment properties and the background PFAS concentrations are provided in Tables S3 and S4.

To perform sorption experiments under contrasting salinities, a series of solutions was prepared by adding different amounts of synthetic sea salt into Milli-Q water, and the salinity was measured by a salinometer and recorded. The pH of each experimental solution was adjusted to 7.8 with 0.1M HCl and 0.1M NaOH solutions. The selected pH reflects the natural conditions in the studied estuarine environment (Munoz et al., 2017) and is commonly employed in PFAS sorption studies to ensure consistent anionic speciation of PFAS as well as stable sediment surface properties (Nguyen et al., 2020; Yin et al., 2022). Please see Table S6 in the Supplementary information for additional details on pH and salinity.

#### **Batch sorption experiments**

Batch sorption experiments were performed in either 50 or 225 mL polypropylene (PP) centrifuge tubes, depending on the SPM concentration. A mixed solution containing eight PFCAs, two PFSAs and one polyfluoroalkyl betaine was prepared in MeOH at 0.3–2.2 µg/L. PFAS with different properties were studied as a mixture, in order to mimic environmental conditions (i.e. co-occurrence of PFAS).

In order to determine the sorption equilibrium time, preliminary sorption kinetic experiments were carried out. Specifically, 25 mg of sediment was weighed into each 50 mL polypropylene (PP) centrifuge tube (i.e. SPM level = 1 g/L), then 50 mL of water (17.5 ‰) was added, and the pH of the experimental solution was adjusted to 7.8. The sediment/water mixtures were equilibrated overnight in a horizontal shaker at 250 rpm and 20 °C. Then, the target PFAS were added to the sample, so that the initial concentration of each PFAS reached 1 nM. At each time interval (2h, 8h, 24h, 48h and 72h), aqueous and sediment phases were separated by centrifugation at 5000 x g for 5 min, then stored at -20°C in polyethylene containers until further analysis. Experiments were run in triplicates.

To investigate the linear range of PFAS sorption isotherms, sorption was first studied under two representative conditions that are prone to exhibit nonlinear isotherms: #1) low S and high SPM concentration (0.15 ‰ and 3000 mg/L, respectively), and #2) high S and low SPM concentration (35 ‰ and 150 mg/L, respectively). The initial PFAS concentrations were in the range 0.17–20 nM (i.e. approximately 0.17 nM, 0.33 nM, 0.83 nM, 1.67 nM, 5 nM, 10 nM and 20 nM). Based on the sorption kinetic study, 24 h was sufficient to reach sorption equilibrium (see below). The sorption isotherm experiments therefore lasted for 24 h, then samples were centrifuged to separate the dissolved and particulate phases as described above.

Based on the results of the preliminary sorption isotherm experiments, we concluded that, when considering the whole PFAS mixture, PFAS sorption was linear over the concentration range of 0.12–1.31 nM (see section 3.2). The combined effects of S and SPM concentration on PFAS sorption were studied within that range, through a 5×7 full factorial experimental design. S varied from 0.15 to 35 % (5 levels: 0.15, 9, 17.5, 26.5, and 35 %,) while SPM ranged between 37.5 and 3000 mg/L (7 levels: 37.5, 80, 150, 350, 750, 1500, and 3000 mg/L). It is noteworthy that tests were performed at PFAS concentrations at least two orders of magnitude lower than those commonly found in the literature, aligning more closely with realistic environmental conditions Full details on S/SPM combinations are provided in Table S8. Experiments were conducted in duplicates with an aqueous PFAS concentration of 0.12–1.31 nM (depending on the compound) and an equilibration time of 24 h; samples were then processed as described above. The order of the experiments was generated randomly using a full factorial design in Minitab software.

#### **PFAS** analysis

Aqueous samples were diluted with MeOH (1:1, v/v), then spiked with 0.8 ng IS standard mixture. Freeze-dried sediment samples (0.0075–0.15 g) with 0.2–8 ng internal standard mixture

were subjected to sonication-assisted extraction with 2 mL of MeOH containing 50 mM ammonium acetate (10 min, 70 °C) before ENVI-Carb cleanup. Extracts were concentrated to 200–700  $\mu$ L at 45 °C under a gentle nitrogen flow.

The quantitative analysis was carried out on a 1290 liquid chromatography system combined with a 6460 triple quadrupole mass spectrometer, both from Agilent Technologies (Massy, France). The system was operated in multi-reaction monitoring mode (MRM) with positive and negative electrospray ionization. The chromatographic separation was completed on Eclipse plus C18 column (1.8m, 2.1mm×100mm; Agilent Technologies, USA). The mobile phase consisted of 2 mM ammonium acetate in water and 95% ACN / 5% water containing 2 mM ammonium acetate (v/v), and the flow rate was set at 0.4 mL/min. Please see Table S2 and Table S6 for full details on MRM mass transitions and instrumental conditions. Internal calibration curves were used to quantify PFAS and R² values of all curves were greater than 0.99.

#### Quality assurance and quality control

Kinetic experiments were carried out in triplicates and isotherm experiments were carried out in duplicates. Control experiments (sediment-free) were carried out to investigate the PFAS loss due to sorption onto PP tube walls, which accounted for 0.3–31 % of the mass initially added, depending on the compound (see Figure S1 and Table S7). In addition, recovery experiments were carried out for both water and sediment samples, to assess the efficiency and reliability of the pretreatment method (Table S7). Limits of detection (LODs) and limits of quantification (LOQs) were defined as the concentration with a signal-to-noise ratio of 3 and 10, respectively (Table S7).

#### Sorption models

In order to figure out the sorption mechanism of PFAS on clay sediment, the sorption kinetics data was fitted by pseudo-second-order model, and the model could be expressed as follows (Miao et al., 2017):

(1) 
$$\frac{t}{q_t} = \frac{1}{k_2 q_e^2} + \frac{t}{q_e}$$

Where  $q_t$  is the amount of PFAS adsorbed on the sediments at time t (h) (ng/mg);  $q_e$  is the amount of PFAS adsorbed on the sediments at equilibrium (ng/mg); k2 is the sorption rate constant (mg/ng/h).

The linearity of sorption isotherms is mainly related to the initial aqueous PFAS concentration, sediment properties and solution characteristics (Chen et al., 2020). Isotherm models, including both nonlinear and linear models, are commonly used for complete information on sorption affinity.

At low initial PFAS aqueous concentrations, PFAS sorption isotherms tend to be linear. It is expressed as (Guo et al., 2016; Miao et al., 2017):

(2) 
$$q_e = K_d C_e$$

Where  $K_d$  (mL/g) is the distribution coefficient of PFAS between sediments and water. At given equilibrium concentrations, the single-point distribution coefficient ( $K_d$ ) could provide information on specific-concentration distribution, which is commonly used for comparing the sorption capacity under different conditions in many studies (Chen et al., 2020).

At higher aqueous PFAS concentrations, however, sorption may deviate from linearity. Hence, more complex models are required to describe PFAS-sediment interactions. The Freundlich isotherm model is frequently used in such cases and can account for the nonlinearity of sorption isotherms by concave and convex patterns (Chen et al., 2020). It is defined as follows (Guo et al., 2016; Miao et al., 2017):

(3) 
$$q_e = K_F C_e^n$$

Where  $q_e$  (ng/mg) and  $C_e$  (ng/mL) are the equilibrium concentrations of PFAS in the solid and aqueous phases, respectively;  $K_F$  (ng/mg)/(ng/mL)n is the capacity affinity parameter; n (dimensionless) is the exponential parameter. When n<1, the nonlinear isotherm exhibits a convex

pattern, which can be explained by the heterogeneity of the sediment and the occurrence of competition for the sorbent (Chen et al., 2020); When n>1, sorption isotherm exhibits a concave pattern, which is induced by solute interactions through the vertical stacking of PFAS alkyl chains. This may lead to cooperative sorption, in addition to interactions with sorption sites of different nature (Chen et al., 2020).

#### Response surface methodology

Response surface methodology (RSM) is an effective experimental design method widely used for investigating the effects and potential interactions between various variables associated with the response (Malyuta et al., 2023).

As described above, a full factorial design was implemented to investigate the combined effects of SPM and S on PFAS sorption (Table S8) The experimental data were evaluated in Minitab 16 software and fitted to the second-order polynomial equation model to determine the influence of these two factors on the Kd of individual PFAS.

The response function, modeled as a second order polynominal function, was determined using regression analysis. The quadratic model was as follows (Hasan et al., 2010):

(4) 
$$Y = \beta_0 + \sum \beta_i X_i + \sum \beta_{ii} X_i^2 + \sum \beta_{ij} X_i X_j + \varepsilon$$

where Y is the response,  $\beta_0$  is the constant,  $\beta_i$  is the slope or linear effect of the input factor  $X_i$ ,  $\beta_{ii}$  is the quadratic effect of input factor  $X_i$ ,  $\beta_{ij}$  is the linear-by-linear interaction effect between the input factor  $X_i$  and  $\epsilon$  is the residual term. Statistical significance was set at p <0.05.

#### Results and discussion

#### **Sorption kinetics**

The sorption kinetics of eleven PFAS onto sediments are shown in Figure 1. It was observed that significant PFAS sorption occurred within the initial 8 h. Then, sorption increased slowly and there were no significant changes in the PFAS concentration in the sediment after 24 h, suggesting that sorption equilibrium was achieved at 24 h. Such results are consistent with previous studies that reported equilibrium times in the range 0.5–24 h (Askeland et al., 2020; Mejia-Avendaño et al., 2020; Miao et al., 2017; Pan et al., 2009; Yin et al., 2022; You et al., 2010). Studies on similar sorbate-sorbent systems have shown that changes in environmental parameters such as salinity may shift the equilibrium sorption amount but do not extend the time required to reach equilibrium (Yin et al., 2022). To ensure the equilibrium sorption of PFAS on sediments at different salinities (0 - 35 %) and different SPM concentrations (37.5–3000 mg/L), the subsequent adsorption experiments were therefore carried out using 24h equilibration time.

The pseudo-second-order model fitted the data well: all R<sup>2</sup> values determined for the kinetics curves were higher than 0.95 (Table S9), suggesting that chemical interaction was possibly involved in the sorption of PFAS on sediment (e.g., anion exchange interaction) (Yu et al., 2009; Maimaiti et al., 2018). Besides, the molecular structure of PFAS may also affect their adsorption kinetics. The concentration of the eleven PFAS in the sediment at equilibrium followed this order: 8:2FTAB>PFDoDA>PFUnDA>PFDA>L-PFOS>PFNA>Br-PFOS>PFOA>PFHpA>PFHxA>PFHxS (Table S9). As expected, longer-chain PFAS exhibited stronger sorption onto sediment compared with shorter-chain PFAS, indicating that hydrophobic interactions were an important driving force for PFAS sorption (Yin et al., 2022). This was especially evident in the carboxylate group (Figure 1a). Besides, PFSAs (i.e., L-PFOS) had higher concentrations in the sediment than PFCAs (PFNA) with the same perfluorocarbon chain length, which could be attributed to the fact that sulfonates are more hydrophobic than carboxylates (Askeland et al., 2020). In addition, the concentration of the zwitterionic 8:2 FTAB was higher than that of anions (i.e., PFNA, L-PFOS and Br-PFOS) with the same perfluorocarbon chain length. This can be attributed to the fact that 8:2 FTAB exhibits both positive and negative charges, which may result in higher affinity for the negatively charged sediment surface, through electrostatic attraction with cation exchange sites (Xiao et al., 2019; Barzen-Hanson et al., 2017).

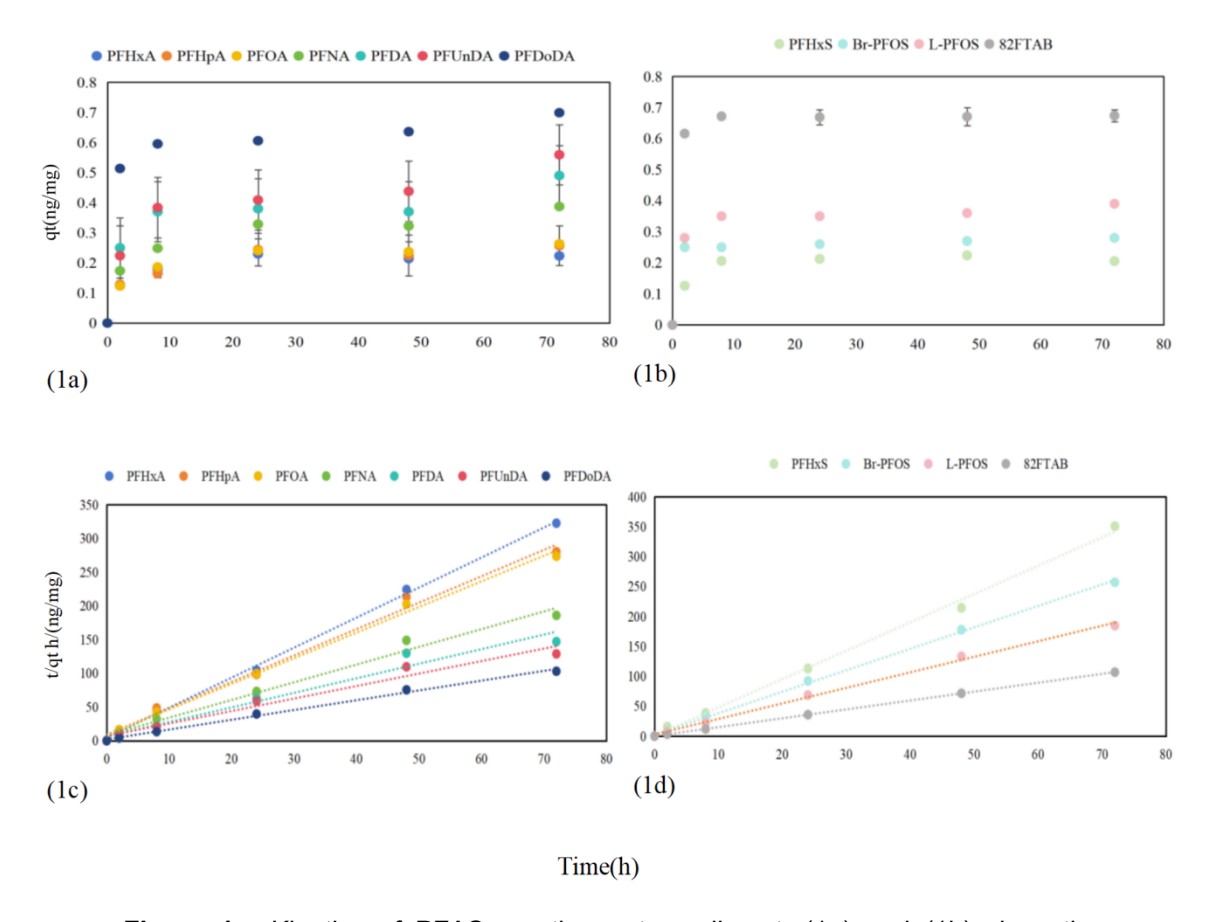


**Figure 1 -** Kinetics of PFAS sorption onto sediment: (1a) and (1b) show the relationships between the sampling time and the PFAS concentrations in the sediment, while (1c) and (1d) show the pseudo-second-order curves.

#### Sorption isotherms

The sorption isotherms of the target PFAS onto sediment were studied using linear and Freundlich models under two conditions (i.e. condition #1: low S + high SPM vs condition #2: high S + low SPM). These contrasting conditions are typical of those found upstream in the fluvial estuary and downstream near the open ocean, respectively. It was hypothesized that lower SPM-water partitioning (i.e. Kd or KF values) were expected under condition #1 compared to condition #2 (Munoz et al., 2017). This phenomenon may be attributed to the fact that elevated SPM concentrations promote particle aggregation, thereby decreasing the specific surface area available for PFAS sorption and ultimately resulting in reduced equilibrium distribution coefficients (Munoz et al., 2017).

For both conditions, it was found that the sorption isotherms of PFAS exhibited both a linear and a non-linear range (Figure 2 and 3).

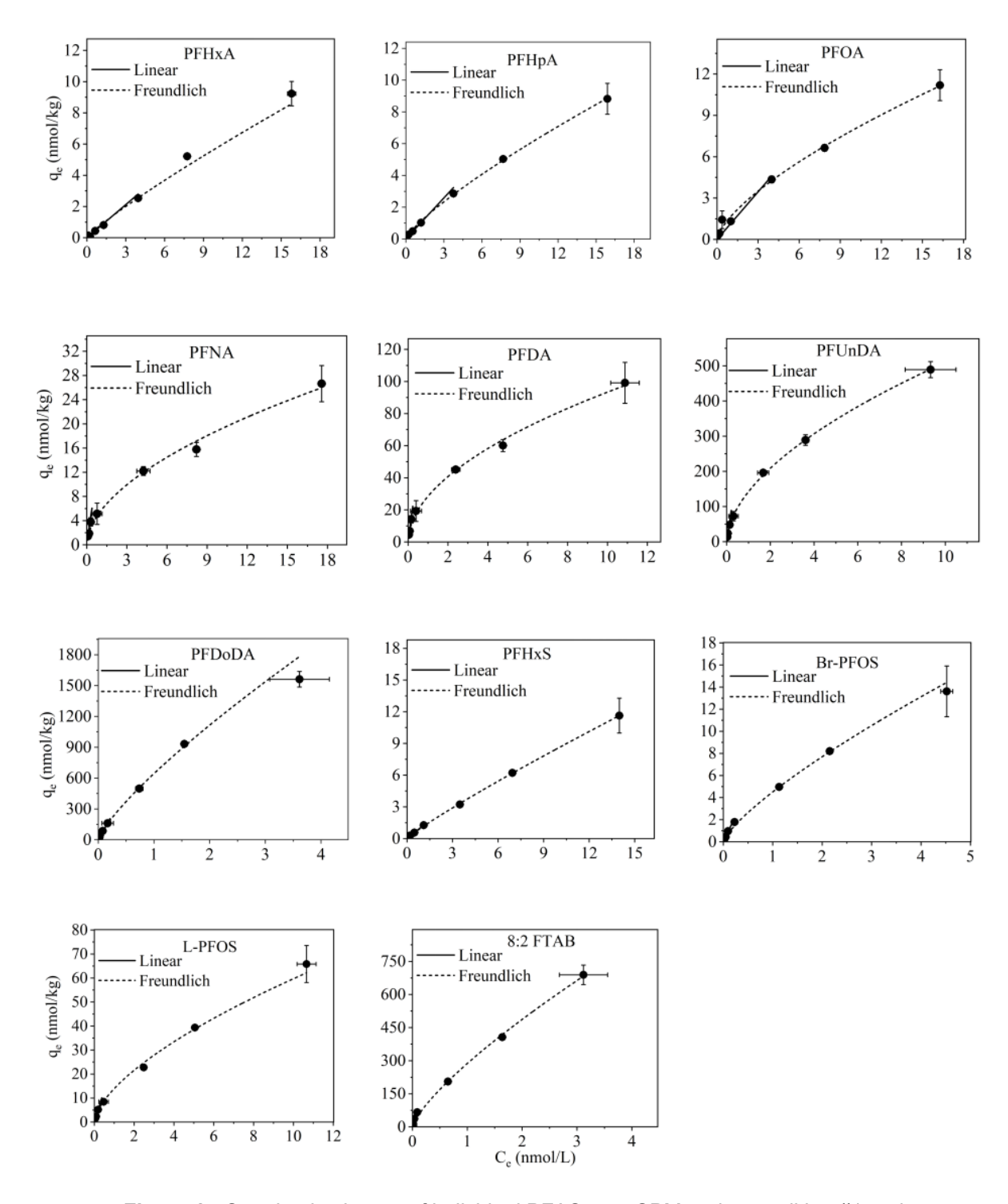


**Figure 2 -** Sorption isotherms of individual PFAS onto SPM under condition #1 and modeling using the Linear and Freundlich models (S: 0.15 %; SPM: 3000 mg/L).

**Table 1 -** Sorption isotherm parameters of PFAS on sediment under conditions #1 and #2. nc: not calculated. Condition #1 (S: 0.15 %; SPM: 3000 mg/L); Condition #2 (S: 35 %; SPM: 150 mg/L)

	<b>Condition 1</b> (S=0.15 ‰,	Condition 1 (S=0.15 ‰, SPM=3000 mg/L)	ıg/L)				Condition 2 (S=35 ‰, SF	Condition 2 (S=35 ‰, SPM=150 mg/L)				
Compounds	Freundlich		Linear	L	_	Linear range	Freundlich		Linear	·	Linear range	range
	c	KF (ng/g)/(ng/ mL) <sup>n</sup>	<u>"</u>	Kd (L/kg)	$\mathbf{A}_2$	Equilibrium concentration min-max (nM)	c	KF (ng/g)/(ng/ mL) <sup>n</sup>	<b>™</b>	Kd (L/kg)	$\Xi_2$	Equilibrium concentration min-max (nM)
PFHxA	0.90±0.06	0.66±0.05	1.00	0.71±0.10	0.93	0.10–3.96	0.97±0.04	1.6±0.1	0.98	1.60±0.08	1.00	0.10–15.22
PFHpA	0.80±0.01	0.80±0.01	1.00	0.86±0.11	0.94	0.08-3.76	0.41±0.04	4.4±0.2	0.97	8.5±0.6	0.98	0.11–1.24
PFOA	$0.68\pm0.04$	1.30±0.08	1.00	1.20±0.13	0.95	0.07-3.48	$0.26\pm0.06$	23.3±3.3	0.91	68.7±4.5	66.0	0.12-1.23
PFNA	$0.54\pm0.03$	3.80±0.02	0.99	15.50±0.03	96.0	0.06-0.95	$0.25\pm0.06$	6746	0.91	292±1	66.0	0.09-0.97
PFDA	$0.52\pm0.02$	21±1	0.99	95.1±1.8	0.97	0.08-0.70	$0.20\pm0.11$	391±6	0.95	856±17	1.00	0.08-0.99
PFUnDA	$0.55\pm0.01$	110±2	1.00	417±10	0.99	0.04-0.36	$0.48\pm0.05$	29∓096	0.95	2295±1	66.0	0.05-0.67
PFDoDA	0.79±0.02	582±21	1.00	965±1	0.99	0.02-0.18	0.68±0.01	3135±112	0.97	6526±4	0.95	0.02-0.26
PFHxS	0.90±0.01	0.99±0.02	1.00	1.20±0.61	1.00	0.05-0.58	0.40±0.04	4.3±0.2	0.99	8.3±4.5	0.98	0.08-0.85
Br-PFOS	0.77±0.01	3.80±0.03	1.00	9.4±2.7	0.99	0.04-0.36	$0.62\pm0.07$	22.3±1.8	0.97	61.7±9.9	66.0	0.04-0.52
L-PFOS	0.63±0.03	10.7±0.7	0.99	26.5±7.2	1.00	0.02-0.12	$0.35\pm0.06$	108±7	06.0	224±12	1.00	0.02-0.26
8:2 FTAB	$0.75\pm0.03$	262±6	1.00	722±43	0.97	0.01-0.15	0.74±0.04	1206±198	0.94	2392±89	66.0	0.01-0.18

As regards condition #1, the linear range is shown in Table 1. At low aqueous equilibrium concentrations, PFAS exhibited linear isotherms that were fitted by the linear model ( $R^2 > 0.93$ ); the Kd values obtained from the slope of the linear isotherms for all PFAS in the concentration ranged from 0.71 to 965 L/kg. At higher aqueous equilibrium concentrations, however, PFAS sorption isotherms reflected nonlinear sorption and they were fitted by the Freundlich model (R<sup>2</sup>>0.99); KF values were in the range of 0.66 to 582 (ng/g)/(ng/mL)<sup>n</sup> (Table 1). Here, the convex pattern of the isotherm curve was attributed to the limited number of sorption sites provided by the sediments even under high SPM concentration, which was also reported by other studies (Chen et al., 2020; Pan et al., 2009; Xiao et al., 2019; You et al., 2010). Results from both the linear and Freundlich models indicated that PFAS structure had an impact on their sorption behavior. Longerchain PFCAs or PFSAs indeed showed greater sorption than their shorter-chain counterparts (i.e., PFDoDA > PFUnDoA > PFDA > PFNA > PFOA > PFHpA > PFHxA and L-PFOS > Br-PFOS > PFHxS). For PFAS of equal fluoroalkyl chain length, sulfonates exhibited stronger sorption than carboxylates (e.g., L-PFOS > PFNA, and PFHxS > PFHpA), and the only zwitterion considered in this study showed greater sorption than anions with a similar number of perfluorinated carbon atoms (e.g., 8:2FTAB > L-PFOS and PFNA). In addition, linear PFAS demonstrated significantly stronger sorption to sediment than their branched counterparts (e.g., L-PFOS vs. Br-PFOS). This difference is attributed to the linear isomers' rod-like conformation, which facilitates extensive van der Waals interactions with the sorbent surface and has been observed previously (e.g., Munoz et al., 2017). Overall, these sorption trends are consistent with previous studies (Xiao et al., 2011; Barzen-Hanson et al., 2017; Nguyen et al., 2020; Mejia-Avendaño et al., 2020; Sharifan et al., 2021).

As expected, results showed that PFAS with higher Kd values were more prone to exhibit non-linear isotherms at lower equilibrium aqueous concentrations compared to those with lower Kd values. PFAS with weaker sorption (i.e. PFHxA, PFHpA and PFHxS) displayed an extended linear range. For these compounds, the results obtained from linear and Freundlich models were close. Indeed, the Kd values were within 107–121 % of the KF values, and the values of n were very close to 1 (0.80–0.90) (Table 1). The isotherms of those PFAS exhibiting stronger sorption at higher concentrations showed larger deviation from linearity, i.e. n values in the range 0.52–0.79. The Kd of these PFAS, as determined in the linear concentration range, were 2.5–4.5 times higher than KF calculated for the whole concentration range.

As regards condition #2, PFAS also exhibited isotherms that could be fitted with a linear model at lower aqueous concentrations ( $R^2 > 0.95$ ). At higher concentrations, however, sorption deviated from linearity and data was fitted well with the Freundlich model for most PFAS (R<sup>2</sup>>0.91). Under condition #2, the linear range spanned from 0.18 to 15.22 nM (Table 1). However, compared with condition #1 and as expected, the sorption of all PFAS was facilitated under condition #2: Kd values ranged between 1.60 and 6526 L/kg, i.e. 2.5-6 times higher than those obtained under condition #1. Similarly, the KF values for all PFAS were in the range 1.62–3135 (ng/g)/(ng/mL)<sup>n</sup>, i.e. 2.5-43 times higher than those obtained under condition #1. A previous study investigating PFAS sorption on sediment under different S reported somewhat smaller KF, in the range 0.88-209 (ng/g)/(ng/mL)<sup>n</sup> for S values between 0 and 30 % (Yin et al., 2022). It is worth noting that the SPM concentration reported in the latter study (125 mg/mL) was much higher than in the present work; higher SPM concentration may provide smaller sorption surface to PFAS due to flocculation and result in lower KF value (Yin et al., 2022). In addition, salting-out is also suspected for PFAS (Hong et al., 2013; Munoz et al., 2017; Yin et al., 2022). This increase in Kd and KF could be attributed to the fact that increased salinity levels are anticipated to lower the electrostatic repulsion between negative charges on PFAS and the overall negatively charged sediment surfaces, such as iron oxides and natural organic matter (i.e. bridging with divalent cations like Ca<sup>2+</sup>or Mg<sup>2+</sup>).

Hence, based on the results obtained under two contrasting representative conditions, the upper limit of the linear sorption range for the studied PFAS was estimated between 0.12 and 1.31 nM depending on the compound. Thus, subsequent tests were performed with PFAS concentrations within this range, so that sorption could be simply assessed through Kd determination.

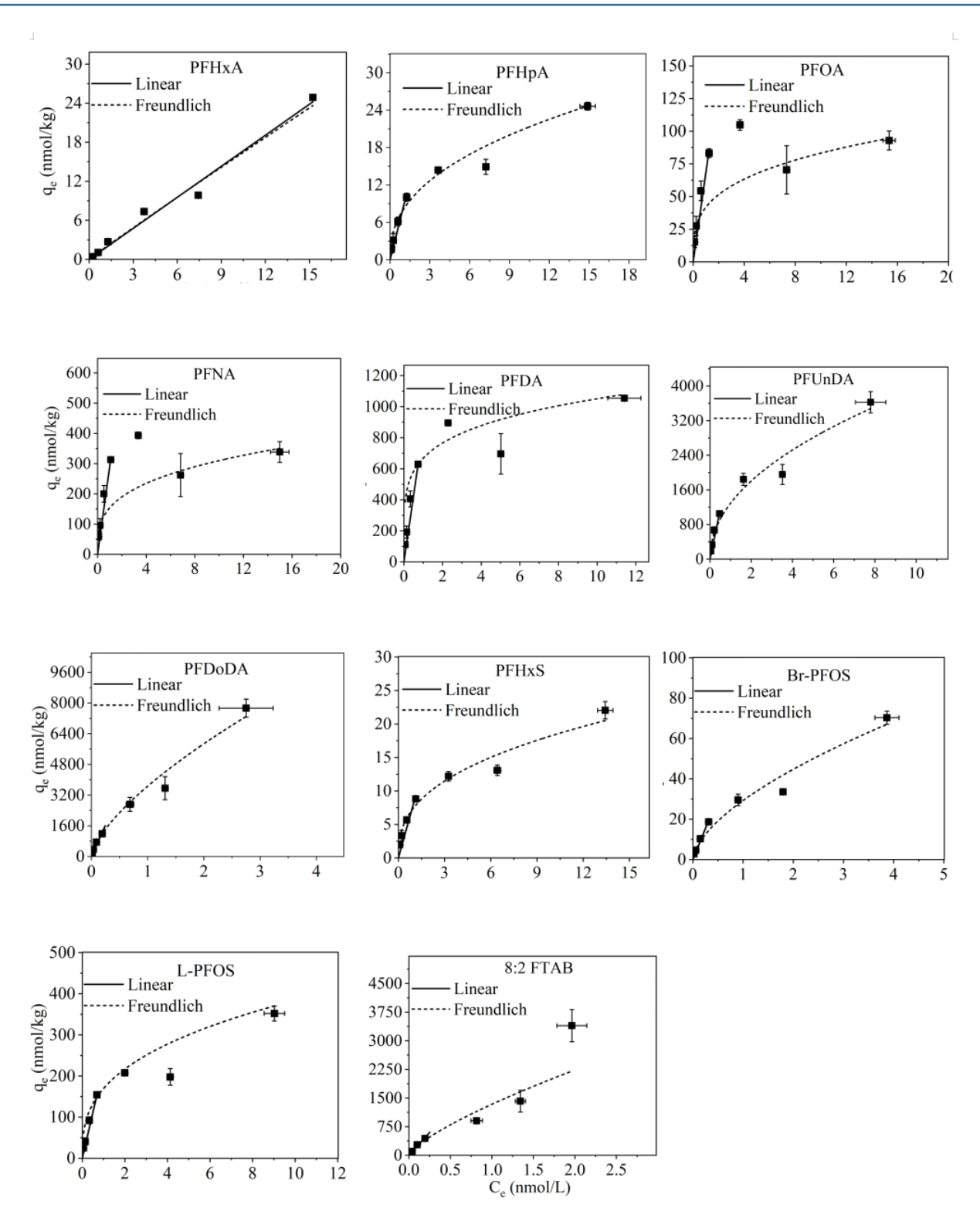


**Figure 3 -** Sorption isotherms of individual PFAS on the sediment under condition #2 (S: 35 %; SPM: 150 mg/L) and modeling using the Linear and Freundlich equations

### Influence of S and SPM on the Kd of PFAS

First, we investigated the combined effect of S and SPM on the Kd of PFAS via regression analysis. The response Kd and the parameter SPM had log-normal distribution, so data was In-

converted prior to multiple regression analysis. A summary of the model coefficients/parameters and regression model equations are presented in Table S10 and Table S11, respectively.

The linear terms of S and In SPM were found significant for all PFAS (p<0.001). In addition, we found that In Kd was positively related to S while it was negatively related to In SPM (Table S11). This confirms that S has a positive effect on Kd due to both salting-out and the reduction of electrostatic repulsion (Hong et al., 2013; Munoz et al., 2017; You et al., 2010) while the decrease of Kd with SPM may be attributed to third phase (i.e. colloid) partitioning which lowers the apparent Kd (see below) (Bowman et al., 2002).

Kd was related to S by a "salting-out" constant (σads\*, L·g<sup>-1</sup>) using the following model:

(5) 
$$K_d 0 = K_d 0 \times e^{2.303 \text{ \sigma ads} * S}$$

with Kd being the relative solubility in saline water and Kd0 being the extrapolated value in freshwater (Turner & Rawling, 2001). The conversion to a molar-based salting-out constant ( $\delta$ , L/mol) was performed. The  $\delta$  values were in the range 0.31–3.96 (Table S12), which is consistent with the in situ values derived by Hong et al. (Hong et al., 2013) at Youngsan and Nakdong river estuaries (South Korea) (SPM =8.1–130 mg/L; S = 0.12–29 ‰;  $\delta$  = 1.34–2.57 L/mol) and by Munoz et al., 2017 in the Gironde estuary (France) (SPM=100–2500 mg/L; S = 2.5–28 ‰;  $\delta$  = 1.79–2.61 L/mol). Considering the different conditions encountered across these studies and the present work (i.e. field vs laboratory-controlled conditions), the difference in  $\delta$  seems reasonable.

The reduction of Kd with increasing SPM was attributed to the particle-concentration effect in previous studies (Bowman et al., 2002; Zhou & Liu, 2000). Interactions between PFAS and colloids could enhance the actual dissolved PFAS concentrations, which may lead to the reduction of apparent Kd (Zhang et al., 2019). Indeed, when sediment concentrations increase, flocculation (i.e. aggregation of particles) may also increase to a certain extent, resulting in a sharp decline in the specific surface area of particles and organic matter available for sorptive interaction (Munoz et al., 2017). In this study, we attempted to assess the colloid mass formed under each experimental condition, using the dry weight method (i.e. oven drying). However, such masses were actually hardly measurable and could not be used as a proxy of colloid concentration in our study (data not shown). Above SPM concentrations of 1.5 g/L, Kd remained relatively constant (Figure 4), suggesting that it is not significantly affected by SPM in high-turbidity environments, such as bottom water (i.e., just above bed sediment).

Overall, In Kd appeared to follow a quadratic model. Coefficients of determination (R²) are presented in Table S10 and regression equations are shown in Table S11. High R² values (0.93–0.96, except for PFHxS: 0.85) and adjusted R² values (0.92–0.96 except for PFHxS: 0.83) indicate that the model Kd prediction was accurate. Apart from R², the low standard deviation of the residuals (0.14–0.52) further indicates that the model may be used to predict PFAS Kd values based on S and SPM data. Plotting predicted vs. actual values (Figure S4 and Table S14) helped interpreting the model adequacy, since the diagnostic plots showed that the data obtained from the model agree well with the experimental data. The actual difference between predicted and actual In Kd values was in the range of 0.85–1.20 L/kg (Table S13).

To further assess the performance of this model, an ANOVA was applied to the dataset (Table S14). The ANOVA confirmed that the two factors (S and SPM) were highly significant (P < 0.05). Pareto charts displayed the standardized effects of variable terms on In Kd in descending order of significance (Figure S2). For PFHxA and PFHpA, SPM exerted a stronger influence on Kd than S. This may be attributed to the relatively high water solubility of short-chain carboxylates and their lower sensitivity to the salting-out effect (Jeon et al., 2011; Munoz et al., 2017). Consequently, their partitioning appears to be more dependent on the available sorption surface than on ionic strength. In contrast, for most other compounds, S emerged as the dominant factor governing Kd values relative to SPM, consistent with their stronger hydrophobicity and greater susceptibility to salting-out (Munoz et al., 2019). Notably, the longer-chain compounds PFUnDA and 8:2 FTAB exhibited nearly equivalent contributions of S and SPM to Kd, a result that remains unexplained and merits further investigation.

To the best of our knowledge, this is the first study that addressed the relative influence of S and SPM and their interaction effect on PFAS sorption onto estuarine sediment, which is crucial for future modeling efforts. In our Kd model, the quadratic terms of S (see equation 4) were positive and significant for the vast majority of PFAS except PFHpA, Br-PFOS and PFDoDA. It was

therefore concluded that S also showed nonlinear effect on Kd for most of the investigated compounds. Conversely, the quadratic terms of In SPM were found to be insignificant (p > 0.05). In addition, the interaction term of S and In SPM was significant or all PFAS except PFUnDA, PFHpA, and 8:2 FTAB, although a p-values close to significance was observed for the latter two compounds. When significant, this interaction term was systematically negative. Figure 4 and figure S3 provide a graphical illustration of this phenomenon: contour lines curve inwards, indicating that increasing one factor reduces the effect of the other. In other words, the effect of SPM on Kd was stronger at high S values, while it was weaker at low S values for most compounds. Such interactions were never evidenced through previous field studies, and our laboratory-based study therefore provides insightful data on this issue.

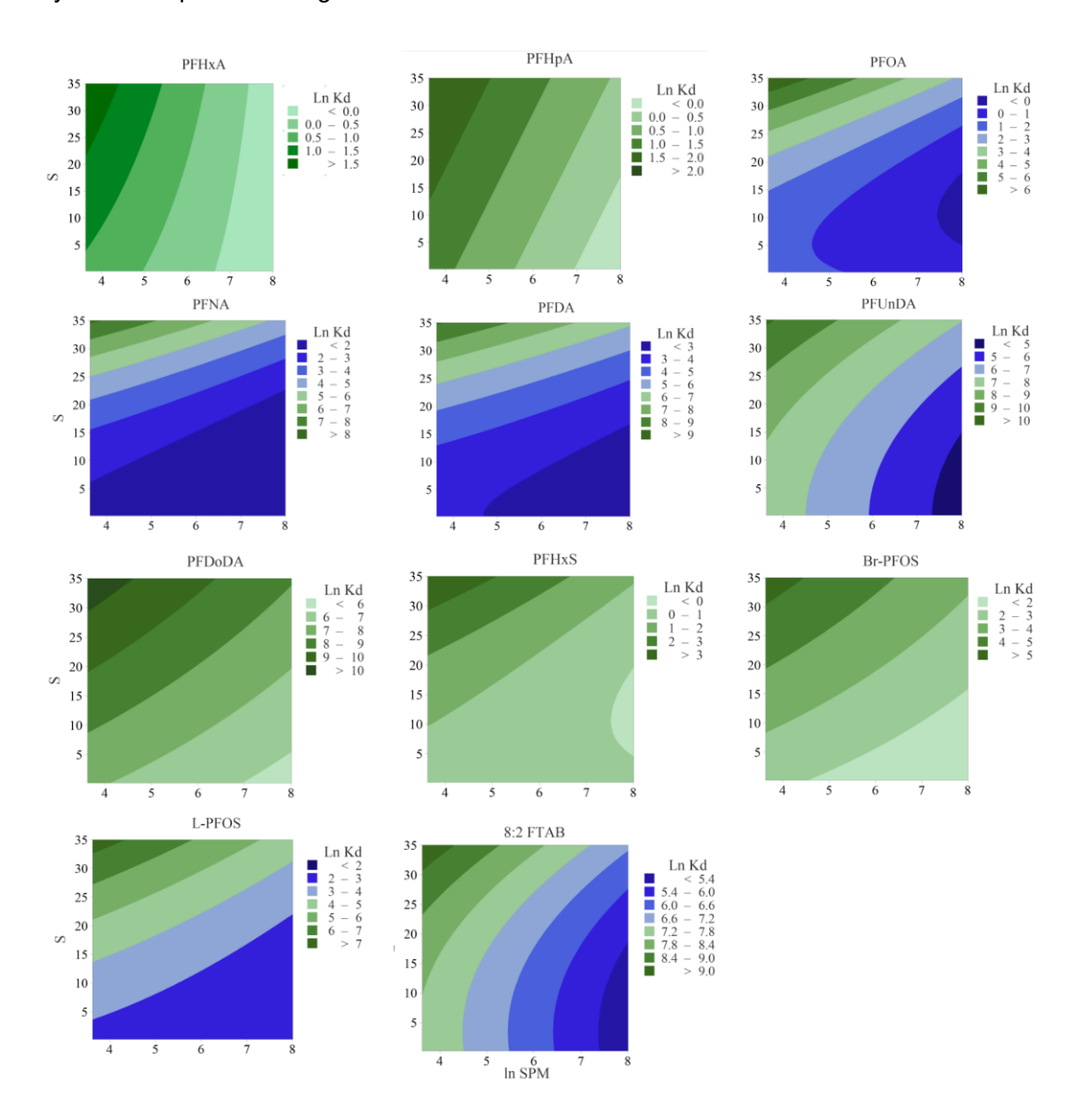


**Figure 4 -** Contour plots showing the influence of salinity (‰) and log-transformed suspended particulate matter (In SPM, mg/L) on the logarithm of partition coefficients (In Kd, L/kg) for 11 native PFAS (including 7 PFCAs and 3 PFSAs and 8:2 FTAB). The plot highlights regions of higher Kd (figured in green) and illustrates how salinity-induced ionic competition and SPM-mediated aggregation affect PFAS partitioning.

#### **Environmental Implications**

The comparison of field data from the Gironde estuary (Munoz et al., 2017) and laboratory-based data (present work) (Table 2) showed that mean log  $K_d$  values for 11 PFAS in the estuarine sediment-water systems were 1.3–8.0 times higher than lab-derived model values. This is consistent with Li et al. (2018), who reported field-derived log  $K_d$  values for PFOS, PFOA, PFNA and PFDA to be 1.6–4.0 times higher than laboratory results. (Zareitalabad et al., 2013) also reported similar discrepancies for short-chain PFAS in coastal systems. This may be explained by several factors, including but not limited to differences in grain size and specific surface. In addition, sorption hysteresis could also be involved. In the Gironde Estuary, decades of PFAS inputs may induce this phenomenon, in which desorption often proves less efficient than adsorption (Xiao et al., 2019). However, many modeling approaches assume reversible sorption, potentially overlooking these hysteresis-related complexities and, as a result, underestimating field-scale PFAS retention (Xiao et al., 2019). Overall, this discrepancy between model-predicted and field-measured  $K_d$  highlights environmental implications for PFAS transport and estuarine risk assessment.

**Table 2 -** Field- versus laboratory-based mean log Kd values of PFAS in the Gironde estuary, with field data from Munoz et al. (2017) and laboratory data from the present study

PFAS	Mean log Kd mean(L/kg)		Kd ratio (Field vs lab)
	Field	Lab	
PFHxA	2.4	0.30	7.95
PFHpA	2.1	0.48	5.69
PFOA	3.3	1.15	2.85
PFNA	3.7	1.86	1.99
PFDA	3.9	2.41	1.61
PFUnDA	3.8	2.89	1.33
PFDoDA	_	3.40	
PFHxS	2.3	0.48	4.84
Br-PFOS	3.5	1.36	2.59
L-PFOS	3.8	1.82	2.10
8:2FTAB	_	2.93	7.95

Our results provide experimental evidence that PFAS Kd values can be influenced by both S and SPM. Consistent with the hypothesis of Munoz et al., (2017), Kd is therefore likely to vary with the seasonal dynamics of the estuarine maximum turbidity zone (MTZ). For instance, PFAS sequestration in estuarine sediments will likely be higher when the MTZ is located near the seaward end of the estuary due to salting-out and intermediate SPM levels. Furthermore, our findings indicate that, for most PFAS, the interaction between S and SPM is negative. This suggests that the salting-out effect is most pronounced at low to intermediate SPM concentrations – typically either upstream or downstream of the MTZ rather than within it.

Finally, this study has several potential limitations that should be acknowledged. First, the model assumes PFAS sorption is fully reversible, ignoring hysteresis and desorption kinetics in estuarine sediments, which could result in underestimating PFAS retention at the field scale. Second, the model was developed using only one sediment (representative of the upper stretch of the Gironde estuary), and our findings should be confirmed for varied estuarine sediment types. Third, although the study covers 7 PFCAs, 3 PFSAs, and 8:2 FTAB, the extrapolation to other PFAS homologues (e.g., fluorinated telomers) requires further validation.

#### **Conclusions**

This study investigated the sorption kinetics of PFAS onto estuarine sediment; this process could be described by a pseudo-second-order model and the equilibrium time for the targeted

PFAS was <24h. Besides, the linear concentration range of PFAS sorption was studied under two representative contrasting conditions: high S and low SPM as well as low S and high SPM. PFAS sorption could be well fitted by linear model for a restricted concentration range (0.12 to 1.31nM at equilibrium) while the Freundlich model proved pivotal for modeling PFAS sorption under an extended concentration range for both conditions. Moreover, a full factorial design was used to investigate the influence of S and SPM on PFAS sorption and their interaction effect. The results showed that both S and SPM were significant factors: Kd was positively related to S due to salting-out effect and decrease of electrostatic repulsion, while it was negatively related to SPM, likely due to flocculation. Additionally, SPM had a stronger effect than S for PFHxA and PFHpA, whereas S was the more dominant factor for most other compounds. For PFUnDA and 8:2 FTAB, S and SPM displayed nearly equivalent weights as drivers of Kd. For the first time, we report on the interaction between S and SPM, which was found to be negative. Through the modelling of PFAS sorption onto estuarine sediment, based on RSM approach, this work definitely provides novel insights into the fate of PFAS at the land-sea interface.

# Acknowledgements

Preprint version 4 of this article has been peer-reviewed and recommended by Peer Community In Ecotoxicology and Environmental Chemistry (https://doi.org/10.24072/pci.ecotoxenvchem.100249; Vignati, 2025). A. Coynel contributed her expertise in sediment pre-treatment. The PLATINE platform (Organic Environmental Analytical Chemistry Platform) at UMR 5805 EPOC provided the analytical facilities dedicated to this project.

## **Funding**

This study has been carried out with financial support CPER A2E (Aquitaine region), E3A (Aquitaine region and FEDER ("Europe is moving in Aquitaine with the European Regional Development Fund (FEDER)") are also acknowledged for funding. C. Gao benefited from a grant awarded by the Chinese Scholarship Council (CSC).

#### Conflict of interest disclosure

The authors declare that they comply with the PCI rule of having no financial conflicts of interest in relation to the content of the article.

# Data, scripts, code, and supplementary information availability

Data are available online: https://doi.org/10.5281/zenodo.15117386 (Gao et al., 2025a) and https://doi.org/10.5281/zenodo.15117401 (Gao et al., 2025b).

Supplementary information is available online: https://doi.org/10.5281/zenodo.16950698 (Gao et al., 2025c).

#### References

Ahmed, M. B., Johir, M. A. H., McLaughlan, R., Nguyen, L. N., Xu, B., & Nghiem, L. D. (2020). Perand polyfluoroalkyl substances in soil and sediments: Occurrence, fate, remediation and future outlook. Science of The Total Environment, 748, 141251. https://doi.org/10.1016/j.scitotenv.2020.141251

Askeland, M., Clarke, B. O., Cheema, S. A., Mendez, A., Gasco, G., & Paz-Ferreiro, J. (2020). Biochar sorption of PFOS, PFOA, PFHxS and PFHxA in two soils with contrasting texture. Chemosphere, 249, 126072. https://doi.org/10.1016/j.chemosphere.2020.126072

Barzen-Hanson, K. A., Davis, S. E., Kleber, M., & Field, J. A. (2017). Sorption of Fluorotelomer Sulfonates, Fluorotelomer Sulfonamido Betaines, and a Fluorotelomer Sulfonamido Amine in National Foam Aqueous Film-Forming Foam to Soil. Environmental Science & Technology, 51(21), 12394–12404. https://doi.org/10.1021/acs.est.7b03452

Bowman, J. C., Zhou, J. L., & Readman, J. W. (2002). Sediment–water interactions of natural oestrogens under estuarine conditions. Marine Chemistry, 77(4), 263–276. https://doi.org/10.1016/S0304-4203(02)00006-3

- Butzen, M. L., Wilkinson, J. T., McGuinness, S. R., Amezquita, S., Peaslee, G. F., & Fein, J. B. (2020). Sorption and desorption behavior of PFOS and PFOA onto a Gram-positive and a Gram-negative bacterial species measured using particle-induced gamma-ray emission (PIGE) spectroscopy. Chemical Geology, 552, 119778. https://doi.org/10.1016/j.chemgeo.2020.119778
- Chen, X.-T., Yu, P.-F., Xiang, L., Zhao, H.-M., Li, Y.-W., Li, H., Zhang, X.-Y., Cai, Q.-Y., Mo, C.-H., & Wong, M. H. (2020). Dynamics, thermodynamics, and mechanism of perfluorooctane sulfonate (PFOS) sorption to various soil particle-size fractions of paddy soil. Ecotoxicology and Environmental Safety, 206, 111105. https://doi.org/10.1016/j.ecoenv.2020.111105
- Du, Z., Deng, S., Bei, Y., Huang, Q., Wang, B., Huang, J., & Yu, G. (2014). Adsorption behavior and mechanism of perfluorinated compounds on various adsorbents—A review. Journal of Hazardous Materials, 274, 443–454. https://doi.org/10.1016/j.jhazmat.2014.04.038
- Evich, M. G., Davis, M. J. B., McCord, J. P., Acrey, B., Awkerman, J. A., Knappe, D. R. U., Lindstrom, A. B., Speth, T. F., Tebes-Stevens, C., Strynar, M. J., Wang, Z., Weber, E. J., Henderson, W. M., & Washington, J. W. (2022). Per- and polyfluoroalkyl substances in the environment. Science, 375(6580), eabg9065. https://doi.org/10.1126/science.abg9065
- Fabregat-Palau, J., Vidal, M., & Rigol, A. (2021). Modelling the sorption behaviour of perfluoroalkyl carboxylates and perfluoroalkane sulfonates in soils. Science of The Total Environment, 801, 149343. https://doi.org/10.1016/j.scitotenv.2021.149343
- Feng, X., Ye, M., Li, Y., Zhou, J., Sun, B., Zhu, Y., & Zhu, L. (2020). Potential sources and sediment-pore water partitioning behaviors of emerging per/polyfluoroalkyl substances in the South Yellow Sea. Journal of Hazardous Materials, 389, 122124. https://doi.org/10.1016/j.jhazmat.2020.122124
- Gao, C., Budzinski, H., Pardon, P., Le Menach, K., & Labadie, P. (2025a). PFAS Kd dataset. Zenodo. https://doi.org/10.5281/zenodo.15117386
- Gao, C., Budzinski, H., Pardon, P., Le Menach, K., & Labadie, P. (2025b). Full Factorial Design Results for the Investigation of PFAS Distribution Coefficient (Kd). Zenodo. https://doi.org/10.5281/zenodo.15117401
- Gao, C., Budzinski, H., Pardon, P., Le Menach, K., & Labadie, P. (2025c). Investigation of the combined influence of salinity and particle concentration on the adsorption of anionic and zwitterionic PFAS onto estuarine sediment using the RSM modelling approach. Supplementary material. Zenodo: https://doi.org/10.5281/zenodo.16950698
- Guo, X., Tu, B., Ge, J., Yang, C., Song, X., & Dang, Z. (2016). Sorption of tylosin and sulfamethazine on solid humic acid. Journal of Environmental Sciences, 43, 208–215. https://doi.org/10.1016/j.jes.2015.10.020
- Hasan, S. H., Srivastava, P., & Talat, M. (2010). Biosorption of lead using immobilized Aeromonas hydrophila biomass in up flow column system: Factorial design for process optimization. Journal of Hazardous Materials, 177(1), 312–322. https://doi.org/10.1016/j.jhazmat.2009.12.034
- Higgins, C. P., & Luthy, R. G. (2006). Sorption of Perfluorinated Surfactants on Sediments. Environmental Science & Technology, 40(23), 7251–7256. https://doi.org/10.1021/es061000n
- Hong, S., Khim, J. S., Park, J., Kim, M., Kim, W.-K., Jung, J., Hyun, S., Kim, J.-G., Lee, H., Choi, H. J., Codling, G., & Giesy, J. P. (2013). In situ fate and partitioning of waterborne perfluoroalkyl acids (PFAAs) in the Youngsan and Nakdong River Estuaries of South Korea. Science of The Total Environment, 445–446, 136–145. https://doi.org/10.1016/j.scitotenv.2012.12.040
- Jeon, J., Kannan, K., Lim, B. J., An, K. G., & Kim, S. D. (2011). Effects of salinity and organic matter on the partitioning of perfluoroalkyl acid (PFAs) to clay particles. Journal of Environmental Monitoring, 13(6), 1803–1810. https://doi.org/10.1039/c0em00791a
- Li, Y., Oliver, D., & Kookana, R. (2018). A critical analysis of published data to discern the role of soil and sediment properties in determining sorption of per and polyfluoroalkyl substances (PFASs). Science Of The Total Environment, 628-629, 110-120. https://doi.org/10.1016/j.scitotenv.2018.01.167
- Liu, C., Chu, J., Cápiro, N. L., Fortner, J. D., & Pennell, K. D. (2022). In-situ sequestration of perfluoroalkyl substances using polymer-stabilized ion exchange resin. Journal of Hazardous Materials, 422, 126960. https://doi.org/10.1016/j.jhazmat.2021.126960

Macorps, N., Labadie, P., Lestremau, F., Assoumani, A., & Budzinski, H. (2023). Per- and polyfluoroalkyl substances (PFAS) in surface sediments: Occurrence, patterns, spatial distribution and contribution of unattributed precursors in French aquatic environments. Science of The Total Environment, 874, 162493. https://doi.org/10.1016/j.scitotenv.2023.162493

- Maimaiti, A., Deng, S., Meng, P., Wang, W., Wang, B., Huang, J., Wang, Y., & Yu, G. (2018). Competitive adsorption of perfluoroalkyl substances on anion exchange resins in simulated AFFF-impacted groundwater. Chemical Engineering Journal, 348, 494–502. https://doi.org/10.1016/j.cej.2018.05.006
- Malyuta, D. A. I., Matteson, K. L., Berry, M. P., Bajwa, D., & Ryan, C. (2023). Experimental statistical modeling of tensile properties and flexural stiffness of recycled high-density polyethylene (rHDPE) thermoplastic using response surface methodology (RSM). Results in Materials, 20, 100472. https://doi.org/10.1016/j.rinma.2023.100472
- Manojkumar, Y., Pilli, S., Rao, P. V., & Tyagi, R. D. (2023). Sources, occurrence and toxic effects of emerging per- and polyfluoroalkyl substances (PFAS). Neurotoxicology and Teratology, 97, 107174. https://doi.org/10.1016/j.ntt.2023.107174
- Mejia-Avendaño, S., Zhi, Y., Yan, B., & Liu, J. (2020). Sorption of Polyfluoroalkyl Surfactants on Surface Soils: Effect of Molecular Structures, Soil Properties, and Solution Chemistry. Environmental Science & Technology, 54(3), 1513–1521. https://doi.org/10.1021/acs.est.9b04989
- Meng, L., Song, B., Zhong, H., Ma, X., Wang, Y., Ma, D., Lu, Y., Gao, W., Wang, Y., & Jiang, G. (2021). Legacy and emerging per- and polyfluoroalkyl substances (PFAS) in the Bohai Sea and its inflow rivers. Environment International, 156, 106735. https://doi.org/10.1016/j.envint.2021.106735
- Miao, Y., Guo, X., Dan Peng, Fan, T., & Yang, C. (2017). Rates and equilibria of perfluorooctanoate (PFOA) sorption on soils from different regions of China. Ecotoxicology and Environmental Safety, 139, 102–108. https://doi.org/10.1016/j.ecoenv.2017.01.022
- Munoz, G., Budzinski, H., Babut, M., Lobry, J., Selleslagh, J., Tapie, N., & Labadie, P. (2019). Temporal variations of perfluoroalkyl substances partitioning between surface water, suspended sediment, and biota in a macrotidal estuary. Chemosphere, 233, 319–326. https://doi.org/10.1016/j.chemosphere.2019.05.281
- Munoz, G., Budzinski, H., & Labadie, P. (2017). Influence of Environmental Factors on the Fate of Legacy and Emerging Per- and Polyfluoroalkyl Substances along the Salinity/Turbidity Gradient of a Macrotidal Estuary. Environmental Science & Technology, 51(21), 12347–12357. https://doi.org/10.1021/acs.est.7b03626
- Munoz, G., Duy, S. V., Labadie, P., Botta, F., Budzinski, H., Lestremau, F., Liu, J., & Sauvé, S. (2016). Analysis of zwitterionic, cationic, and anionic poly- and perfluoroalkyl surfactants in sediments by liquid chromatography polarity-switching electrospray ionization coupled to high resolution mass spectrometry. Talanta, 152, 447–456. https://doi.org/10.1016/j.talanta.2016.02.021
- Munoz, G., Giraudel, J.-L., Botta, F., Lestremau, F., Dévier, M.-H., Budzinski, H., & Labadie, P. (2015). Spatial distribution and partitioning behavior of selected poly- and perfluoroalkyl substances in freshwater ecosystems: A French nationwide survey. Science of The Total Environment, 517, 48–56. https://doi.org/10.1016/j.scitotenv.2015.02.043
- Nguyen, T. M. H., Bräunig, J., Thompson, K., Thompson, J., Kabiri, S., Navarro, D. A., Kookana, R. S., Grimison, C., Barnes, C. M., Higgins, C. P., McLaughlin, M. J., & Mueller, J. F. (2020). Influences of Chemical Properties, Soil Properties, and Solution pH on Soil–Water Partitioning Coefficients of Per- and Polyfluoroalkyl Substances (PFASs). Environmental Science & Technology, 54(24), 15883–15892. https://doi.org/10.1021/acs.est.0c05705
- Pan, G., Jia, C., Zhao, D., You, C., Chen, H., & Jiang, G. (2009). Effect of cationic and anionic surfactants on the sorption and desorption of perfluorooctane sulfonate (PFOS) on natural sediments. Environmental Pollution, 157(1), 325–330. https://doi.org/10.1016/j.envpol.2008.06.035
- Sha, B., Johansson, J. H., Tunved, P., Bohlin-Nizzetto, P., Cousins, I. T., & Salter, M. E. (2022). Sea Spray Aerosol (SSA) as a Source of Perfluoroalkyl Acids (PFAAs) to the Atmosphere: Field Evidence from Long-Term Air Monitoring. Environmental Science & Technology, 56(1), 228–238. https://doi.org/10.1021/acs.est.1c04277

Sharifan, H., Bagheri, M., Wang, D., Burken, J. G., Higgins, C. P., Liang, Y., Liu, J., Schaefer, C. E., & Blotevogel, J. (2021). Fate and transport of per- and polyfluoroalkyl substances (PFASs) in the vadose zone. Science of The Total Environment, 771, 145427. https://doi.org/10.1016/j.scitotenv.2021.145427

- Sorengard, M., Kleja, D. B., & Ahrens, L. (2019). Stabilization of per- and polyfluoroalkyl substances (PFASs) with colloidal activated carbon (PlumeStop®) as a function of soil clay and organic matter content. Journal of Environmental Management, 249, 109345. https://doi.org/10.1016/j.jenvman.2019.109345
- Sörengård, M., Östblom, E., Köhler, S., & Ahrens, L. (2020). Adsorption behavior of per- and polyfluoralkyl substances (PFASs) to 44 inorganic and organic sorbents and use of dyes as proxies for PFAS sorption. Journal of Environmental Chemical Engineering, 8(3), 103744. https://doi.org/10.1016/j.jece.2020.103744
- Turner, A., & Rawling, M. C. (2001). The influence of salting out on the sorption of neutral organic compounds in estuaries. Water Research, 35(18), 4379–4389. https://doi.org/10.1016/S0043-1354(01)00163-4
- Vignati, D. A. L. (2025) Laboratory investigations offer new insights on how salinity and suspended matter concentration jointly affect the solid-to-water partitioning of PFAS in estuaries. *Peer Community in Ecotoxicology and Environmental Chemistry,* 100249. https://doi.org/10.24072/pci.ecotoxenvchem.100249
- Xiao, F., Jin, B., Golovko, S. A., Golovko, M. Y., & Xing, B. (2019). Sorption and Desorption Mechanisms of Cationic and Zwitterionic Per- and Polyfluoroalkyl Substances in Natural Soils: Thermodynamics and Hysteresis. Environmental Science & Technology, 53(20), 11818–11827. https://doi.org/10.1021/acs.est.9b05379
- Xiao, F., Zhang, X., Penn, L., Gulliver, J. S., & Simcik, M. F. (2011). Effects of Monovalent Cations on the Competitive Adsorption of Perfluoroalkyl Acids by Kaolinite: Experimental Studies and Modeling. Environmental Science & Technology, 45(23), 10028–10035. https://doi.org/10.1021/es202524y
- Yin, C., Pan, C.-G., Xiao, S.-K., Wu, Q., Tan, H.-M., & Yu, K. (2022). Insights into the effects of salinity on the sorption and desorption of legacy and emerging per-and polyfluoroalkyl substances (PFASs) on marine sediments. Environmental Pollution, 300, 118957. https://doi.org/10.1016/j.envpol.2022.118957
- You, C., Jia, C., & Pan, G. (2010). Effect of salinity and sediment characteristics on the sorption and desorption of perfluorooctane sulfonate at sediment-water interface. Environmental Pollution, 158(5), 1343–1347. https://doi.org/10.1016/j.envpol.2010.01.009
- Yu, Q., Zhang, R., Deng, S., Huang, J., & Yu, G. (2009). Sorption of perfluorooctane sulfonate and perfluorooctanoate on activated carbons and resin: Kinetic and isotherm study. Water Research, 43(4), 1150–1158. https://doi.org/10.1016/j.watres.2008.12.001
- Zareitalabad, P., Siemens, J., Hamer, M., & Amelung, W. (2013). Perfluorooctanoic acid (PFOA) and perfluorooctanesulfonic acid (PFOS) in surface waters, sediments, soils and wastewater A review on concentrations and distribution coefficients. Chemosphere, 91(6), 725–732. https://doi.org/10.1016/j.chemosphere.2013.02.024
- Zhang, D. Q., Zhang, W. L., & Liang, Y. N. (2019). Adsorption of perfluoroalkyl and polyfluoroalkyl substances (PFASs) from aqueous solution—A review. Science of The Total Environment, 694, 133606. https://doi.org/10.1016/j.scitotenv.2019.133606
- Zhang, Y., Thomas, A., Apul, O., & Venkatesan, A. K. (2023). Coexisting ions and long-chain perand polyfluoroalkyl substances (PFAS) inhibit the adsorption of short-chain PFAS by granular activated carbon. Journal of Hazardous Materials, 460, 132378. https://doi.org/10.1016/j.jhazmat.2023.132378
- Zhong, H., Zheng, M., Liang, Y., Wang, Y., Gao, W., Wang, Y., & Jiang, G. (2021). Legacy and emerging per- and polyfluoroalkyl substances (PFAS) in sediments from the East China Sea and the Yellow Sea: Occurrence, source apportionment and environmental risk assessment. Chemosphere, 282, 131042. https://doi.org/10.1016/j.chemosphere.2021.131042
- Zhou, J. L., & Liu, Y. P. (2000). Kinetics and equilibria of the interactions between diethylhexyl phthalate and sediment particles in simulated estuarine systems. Marine Chemistry, 71(1), 165–176. https://doi.org/10.1016/S0304-4203(00)00047-5